Digital Predistortion with Low-Precision ADCs

Chance Tarver and Joseph R. Cavallaro
Department of Electrical and Computer Engineering, Rice University, Houston, TX
Email: tarver@rice.edu cavallar@rice.edu

***Abstract*—Digital Predistortion (DPD) is a popular technique for linearizing a power amplifier (PA) to help reduce the spurious emissions and spectral regrowth. DPD requires the learning of the inverse PA nonlinearities by training on the output of the PA. In practical systems, the analog output of the PA will have to go through an analog-to-digital converter (ADC) so that training can be done on a digital processor. The quantization degrades signal quality and may limit the performance of a DPD learning algorithm. However, a lower resolution ADC may cost less and allow for less computational complexity in the digital processing. We study this trade-off to try to find how much precision is needed in DPD systems and discover that for a full-band DPD as few as 6 bits can reliably be used. For sub-band DPD, a single bit ADC can be used.**

I. Introduction

The power amplifier (PA) is a component of wireless systems that has a nonlinear transfer function. The nonlinearities are undesirable in that they lead to distortions such as spectral regrowth around the main carriers and intermodulation distortions (IMDs) in scenarios with multiple, noncontiguous carriers such as carrier aggregation (CA) in LTE-Advanced. This is exacerbated in modern, multi-carrier modulations such as OFDMA which have a high peak-to-average power ratio (PAPR).

Digital predistortion (DPD) is a method for linearizing a power amplifier (PA). With DPD, the nonlinearities are estimated so that they can be corrected before the PA with their inverse. To do this, we must train our predistorter by observing the signal after the PA. In practical situations, we need a feedback path after the PA that has a downconverter and an ADC. Typically, DPD bandwidth is five times the signal bandwidth [1]. Hence, for wide bandwidth signals, the sampling rate of the ADC must be fast.

In mobile applications where power and cost are concerns, one option for reducing the complexity of the system is to use a low-precision ADC. By reducing the precision, the DPD algorithm can be performed with shorter word lengths which would save area and power in an implementation. Low precision ADCs often consume less power and support faster sampling rates than higher precision devices [2]. Moreover, these ADC are often cheaper.

For these reasons, the use of low-precision ADCs is being considered in multiple emerging areas of communications. For example, in massive MIMO resolutions as low as a single bit are being considered to help alleviate the data throughput requirements when hundreds of antennas are being used simultaneously [3]. In mmWave, there are large bandwidths available that could enable fast data rates. This necessitates the use of ADCs with fast sampling rates. Again, low-precision ADCs are being considered for this application to reduce the system complexity and power requirements [4].

In this paper, we test the performance of our previous DPD solutions for varying ADC precision. By doing so, we alter the resolution of the feedback path to the DPD learning. As we remove bits, we increase quantization noise which we expect to limit performance. What we find is that a significant number of bits can be removed before there is a significant impact on performance.

The paper is organized as follows. Section II presents a simulation where we reduce the precision on a full-band DPD. In Section III, we repeat the simulation with a sub-band DPD. In Section IV, we perform the sub-band DPD using a SDR to get real hardware results. We then conclude the paper in Section V.

II. Full-Band DPD

Most DPD is a variation of what we refer to as full-band DPD where the entire transmit band near the main carriers is linearized. This can reduce the magnitude of multiple spurious emissions such as the third and fifth intermodulation products and the spectral regrowth around the main carriers. However, this comes with a considerable computational complexity especially as the spacing between the carriers becomes large [5] which also has the negative effect of increasing power consumption and cost in the ADC.

Using a previously developed DPD system [6], we illustrate the effect of quantization in Figure 1. Here, we have two noncontiguous signals like what may be found in LTE-Advanced carrier aggregation. They are each 5 MHz in bandwidth. They are broadcast through a fifth-order, nonlinear PA model with memory effects implemented in MATLAB. Intermodulation occurs and introduces large spurious emissions through the nearby spectrum as seen by the black curve.

A block diagram of the simulation is shown in Figure 2. Currently, all computation is done in double precision. However, at the feedback input to the DPD learning, we quantize using the fixed-point toolbox. Word lengths are varied from an unquantified sixty-four bit double all the way to two bits. When we perform the DPD algorithm where the

This work was supported in part by the US National Science Foundation under grants CNS-1265332 (WiFiUS Program), ECCS-1408370, and CNS-1717218.

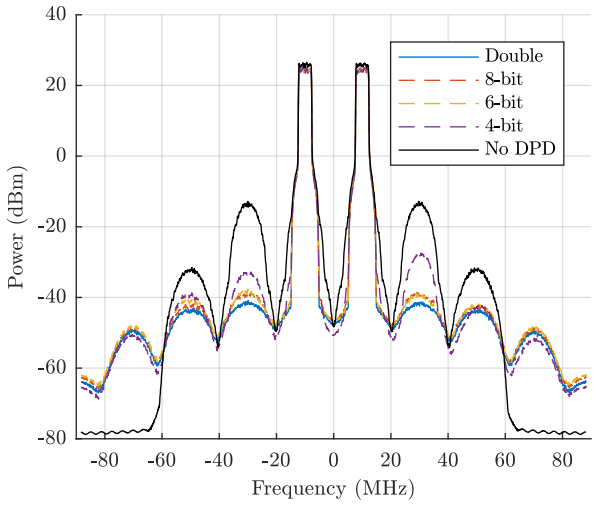

Fig. 1. PSD output when performing full-band DPD on a scenario with two, noncontiguous, 5 MHz LTE uplink carriers with a low-precision ADC feedback path. Here, performance for the 8 bit and 6 bit ADCs are similar with about 2 dB less IM3 suppression when compared to the double-precision PA simulation.

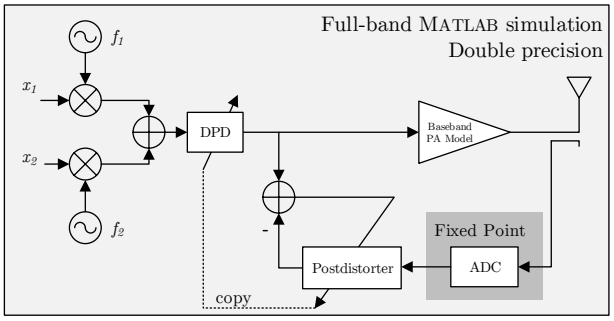

Fig. 2. Block diagram of the full-band DPD simulation performed. The signal generation, amplification, indirect DPD learning, and DPD application are performed with double precision in MATLAB. We emulate an ADC by quantizing the feedback from the PA to the DPD learning.

feedback into the DPD learning block is the full, double-precision values computed by MATLAB, we get suppression shown by the solid blue curve in Figure 1. We then use signed, fixed-point representation. This introduces quantization noise and degrades the performance. However, for as low as 6-bit ADC, the performance degradation is mostly insignificant. For example, there is only a 2 dB difference in suppression on the right-hand IM3 spur. The 4-bit ADC still suppress throughout the spectrum, but there is a significant performance degradation (14 dB on the right-hand IM3).

Here, we are limited by the available dynamic range of the low precision. As we reduce the bits, the noise floor of the feedback raises due to quantization noise. The ADC becomes saturated by the power of the main carriers and simply can not see the relatively low-power signals of the spurious emissions.

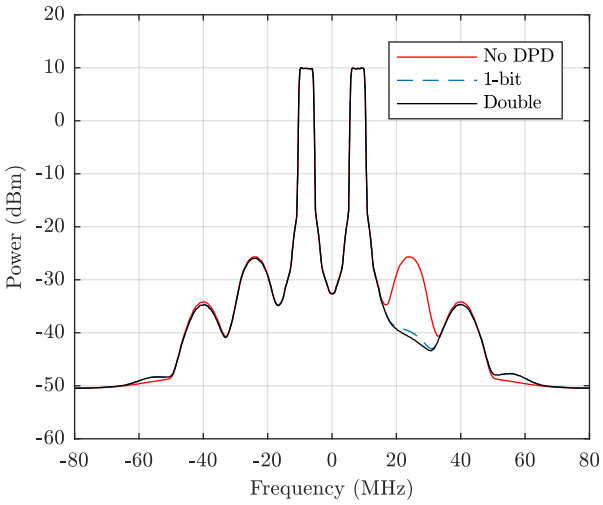

Fig. 3. PSD output when performing sub-band DPD on the IM3+ spur. We use a scenario with two, noncontiguous, 5 MHz LTE uplink carriers with a 1 bit ADC feedback path. Here, performance for the single bit observations has about 2 dB less IM3 suppression when compared to the double-precision PA simulation.

III. SUB-BAND DPD

An alternative to the full-band DPD is what the authors refer to as sub-band DPD. With this method, one targets specific sub-bands such as prominent intermodulation products for suppression. This has the effect of drastically reducing sample rates which in turn reduces the running complexity of the algorithm. This method also provides freedom in the sense that specific sub-bands can be targeted as needed.

Using a previously developed sub-band DPD system [5] we illustrate the effect of quantization in Figure 3. Similar to the full-band simulation in the previous section, we simulate two noncontiguous signals. They are each 5 MHz in bandwidth broadcast through a fifth-order PA model. In the nearby spectrum, there are spurious emissions caused by intermodulation. We use the sub-band DPD method to target the right-hand, third-order intermodulation (IM3+) spurious emission.

When using the sub-band method, it is not necessary to receive the main carriers in the feedback path. Instead, a sub-band DPD can be designed as follows. The RF downconverter can be tuned to the specific frequency of a problematic spurious emission. Then, an analog low-pass filter (LPF) can be used for anti-aliasing and attenuation of the higher-power main carriers. By doing this, we can better use the low dynamic-range available when using a low-precision ADC to receive just the spurious emission. This will provide better performance in the DPD learning algorithm. The block diagram of the proposed system and how it was simulated is shown in Figure 4.

When we perform the third and fifth-order DPD algorithm where the feedback into the DPD learning block is the full, double-precision values computed by MATLAB, we get suppression shown by the solid black curve in Figure 3. We then

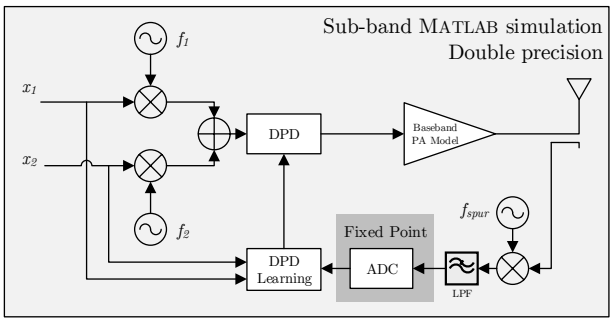

Fig. 4. Block diagram of the sub-band DPD simulation performed. Here, we tune the feedback receiver to the frequency of the spur and pass it through a low-pass filter. The frequency shift, low-pass filtering, signal generation, amplification, DPD learning, and DPD application are performed with double precision in MATLAB. We emulate an ADC by quantizing the feedback from the PA to the DPD learning.

use MATLAB's fixed point toolbox to convert the values to a signed, fixed-point representation. This introduces quantization noise and degrades the performance. However, for as low as a single-bit ADC, the performance degradation is mostly insignificant. For example, there is only a 2 dB difference in suppression on the right-hand IM3 spur.

This creates an exciting opportunity for reducing the complexity of the hardware necessary for a system using the sub-band DPD algorithm. The RF downconverter can be a lower-cost, smaller-bandwidth device since only a sub-band needs to be used for training. The ADC can be replaced by a comparator. This has the effect of reducing area and power overhead which is attractive for mobile devices. This can also be attractive for massive MIMO basestations where DPD computations may need to be done for each of the many RF transmit chains.

The algorithmic complexity can also be reduced. The sub-band DPD learning algorithm is accomplished in [5] via an LMS adaptive training. A version of this is shown below,

$$\alpha^*(n+1) = \alpha^*(n) - \frac{\mu}{|u(n)||^2 + C} e^*(n)u(n). \qquad (1)$$

Here α is the DPD coefficient, $e(n)$ is the error signal vector of a spur at the PA output, $u(n)$ is the LMS reference signal, μ is the LMS learning rate, and n denotes the sample index. The DPD application is achieved by adding a term to the PA input,

$$\tilde{x}(n) = x(n) + [\alpha \star u(n)]\, e^{j2\pi \frac{f_{spur}}{f_s} n}. \qquad (2)$$

The complex multiplication of the error signal by the reference signal in Equation 1, can be simplified when the error signal is only 1-bit. The multiplication can be replaced with sign changes and additions to $u(n)$. This reduces the complexity which helps simplify the implementation of the learning algorithm.

Using this training algorithm, the DPD coefficients are updated iteratively. The convergence of these coefficients for the simulation in this section is shown in Figure 5. Here we show the single-bit case. We see that the third and fifth-order DPD coefficients each converge smoothly despite the low dynamic-range of the feedback path. This is because the LMS update to the coefficient shown in Eq. (1) is simply a small step. To have a smooth convergence, each step needs to only be in the correct direction. For this, the single-bit error signal, $e(n)$, needs only be correlated to the LMS reference signal $u(n)$. Although the error-signal is boxy due to the low precision, it is still correlated to the LMS signal similar to the full-precision case.

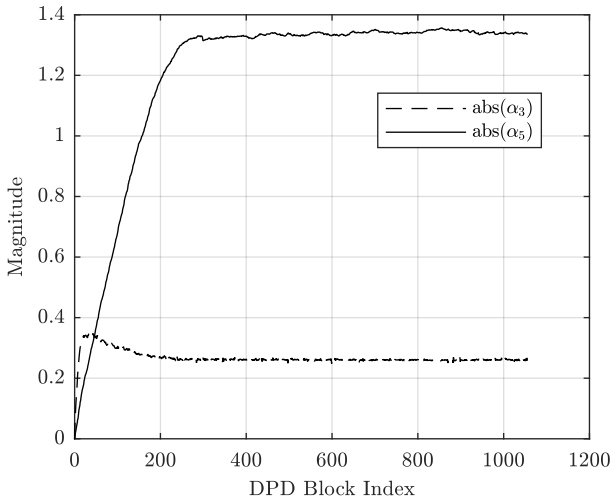

Fig. 5. Convergence of the third and fifth-order DPD coefficients for a single-bit ADC feedback path. Despite having low dynamic range, the error signal is still correlated to the LMS reference signal allowing for smooth LMS convergence.

IV. HARDWARE TESTING

To test the feasibility of performing DPD with fewer bits, we used a WARPv3 software-defined radio board [7]. This is a board that has a WiFi chipset and a power amplifier. We use the WARPLab framework which allows us to use MATLAB to interface with the board. The host PC does all of the signal processing and DPD. A figure of this test setup is shown in Figure 6. Here, we transmit from one RF port and feedback to the other RF port via a directional coupler.

We test the Subband DPD on the WARP board with varying ADC resolutions. The WARPv3 board natively has a 12 bit ADC. For our testing, we emulate a lower precision by simply quantizing the received signal in MATLAB. Since the board only has a bandwidth of 40 MHz, we send two 1.4 MHz LTE uplink carriers discontiguously. The carriers intermodulate due to the nonlinearities in the PA.

We use the same DPD processing as in Section III and account for the third and fifth order nonlinearities in the IM3+ spurious emission. We see the result of the training in Figure 7. The single-bit DPD has only about 1 dB worse performance when compared to the double-precision DPD training. The

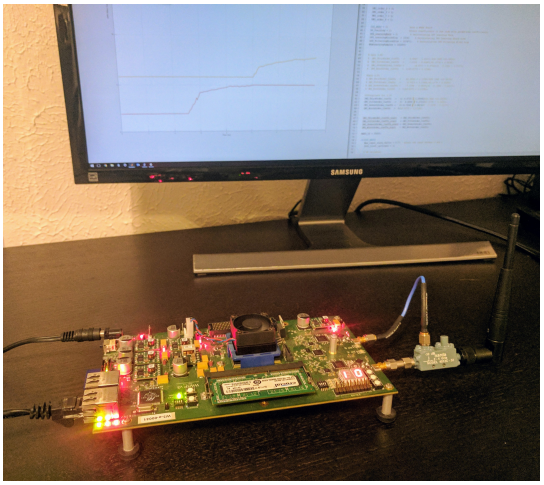

Fig. 6. WARPLab setup for hardware testing. The PC generates samples and performs DPD processing. The WARPv3 transmits with feedback to an RX port using a directional coupler.

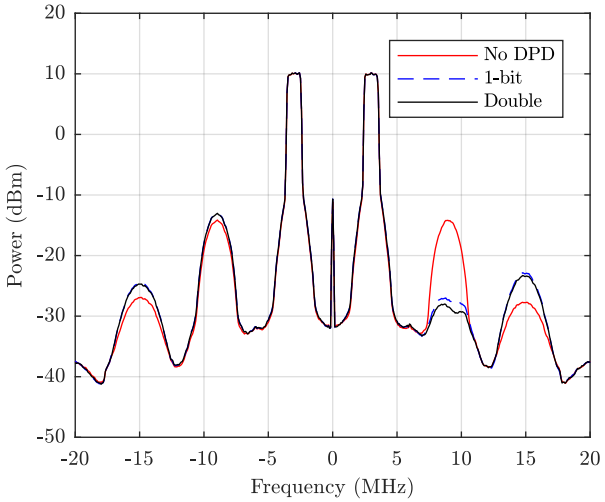

Fig. 7. PSD output when performing sub-band DPD on the IM3+ spur using WARPLab hardware. We use a scenario with two, noncontiguous, 1.4 MHz LTE uplink carriers with a 1-bit ADC feedback path. Here, performance for the single bit observations has about 2 dB less IM3 suppression when compared to the double-precision.

convergence of the DPD coefficients for the 1-bit training can be seen in Figure 8.

V. Conclusion

Digital predistortion is a valuable method to linearize PAs that does not necessarily need to be computationally costly or require complicated hardware overhead. When designing a system with DPD, one consideration should be the precision of the ADC. With a low-precision ADC of about four or six bits, the performance of the full-band DPD training can remain mostly intact. With a sub-band DPD, a single bit is sufficient for a decent suppression of a single spurious emission. This is an attractive option for linearization on handsets where power

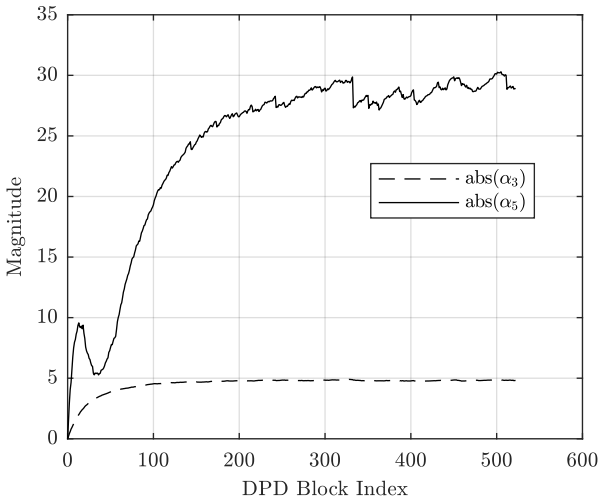

Fig. 8. Convergence of the third and fifth-order DPD coefficients for a single-bit ADC feedback path in the WARPLab hardware experiments.

is of concern or in massive MIMO where it may be inefficient to perform a full resolution DPD for every transmit chain.

References

[1] A. Katz, J. Wood, and D. Chokola, "The Evolution of PA Linearization: From Classic Feedforward and Feedback Through Analog and Digital Predistortion," *IEEE Microwave Magazine*, vol. 17, no. 2, pp. 32–40, 2016. [Online]. Available: https://doi.org/10.1109/MMM.2015.2498079

[2] R. H. Walden, "Analog-to-digital converter survey and analysis," *IEEE Journal on Selected Areas in Communications*, vol. 17, no. 4, pp. 539–550, 1999. [Online]. Available: https://doi.org/10.1109/49.761034

[3] S. Jacobsson, G. Durisi, M. Coldrey, U. Gustavsson, and C. Studer, "Throughput analysis of massive mimo uplink with low-resolution adcs," *IEEE Transactions on Wireless Communications*, vol. 16, no. 6, pp. 4038–4051, June 2017. [Online]. Available: http://dx.doi.org/10.1109/TWC.2017.2691318

[4] C. Rusu, R. Mendez-Rial, N. Gonzalez-Prelcic, and R. W. Heath, "Adaptive One-Bit Compressive Sensing with Application to Low-Precision Receivers at mmWave," in *2015 IEEE Global Communications Conference (GLOBECOM)*, 2015, pp. 1–6. [Online]. Available: http://dx.doi.org/10.1109/GLOCOM.2015.7417853

[5] M. Abdelaziz, L. Anttila, C. Tarver, K. Li, J. R. Cavallaro, and M. Valkama, "Low-Complexity Subband Digital Predistortion for Spurious Emission Suppression in Noncontiguous Spectrum Access," *IEEE Transactions on Microwave Theory and Techniques*, vol. 64, no. 11, pp. 3501–3517, 2016. [Online]. Available: https://doi.org/10.1109/TMTT.2016.2602208

[6] K. Li, A. Ghazi, C. Tarver, J. Boutellier, M. Abdelaziz, L. Anttila, M. Juntti, M. Valkama, and J. R. Cavallaro, "Parallel Digital Predistortion Design on Mobile GPU and Embedded Multicore CPU for Mobile Transmitters," *Journal of Signal Processing Systems*, vol. 89, no. 3, pp. 417–430, Dec 2017. [Online]. Available: https://doi.org/10.1007/s11265-017-1233-y

[7] "WARP Project." [Online]. Available: http://warpproject.org